

## Corrosion protection of NdFeB magnets by phosphating with tungstate incorporation

S.M. Tamborim Takeuchi<sup>a</sup>, D.S. Azambuja<sup>a,\*</sup>, A.M. Saliba-Silva<sup>b</sup>, I. Costa<sup>b</sup>

<sup>a</sup> Instituto de Química, Universidade Federal do Rio Grande do Sul, RS, CEP 91501-970, Porto Alegre-RS, Brazil

<sup>b</sup> Instituto de Pesquisas Energéticas e Nucleares, IPEN/CNEN-SP, Brazil

Received 14 January 2005; accepted in revised form 18 October 2005

Available online 15 December 2005

### Abstract

In this investigation the effect of surface treatments on the corrosion resistance of a commercial NdFeB sintered magnet has been investigated. A solution of  $10 \text{ g L}^{-1}$   $\text{NaH}_2\text{PO}_4$ , acidified to pH 3.8 has been used for phosphating this magnet. The corrosion resistance of the phosphated magnet was investigated in a  $0.10 \text{ mol L}^{-1}$   $\text{Na}_2\text{SO}_4$  solution by electrochemical impedance spectroscopy and cyclic voltammetry with rotating disc electrode. The obtained results reveal that the resistance decreases with exposure time due to the development of pores and/or defects in the conversion coating exposing the substrate to corrosive attack. The effect of tungstate incorporation into the phosphate conversion coating resulting from a phosphating treatment prior to immersion in the tungstate solution was evaluated. The proposed treatment consists of re-immersing the phosphated samples in a  $0.1 \text{ mol L}^{-1}$   $\text{Na}_2\text{WO}_4$  solution during 72 h at the open circuit potential (OCP). Under these conditions, the corrosion resistance of the magnet was improved and this was attributed to the formation of a protective layer due to the adsorption of tungstate anions at the metallic substrate exposed in the coating, decreasing metal dissolution.

© 2005 Published by Elsevier B.V.

**Keywords:** Phosphating; Corrosion protection; NdFeB; Tungstate conversion layer

### 1. Introduction

NdFeB magnets are technologically important materials for efficient use of electrical energy. Unfortunately, sintered NdFeB magnets are highly susceptible to corrosion in various environments [1–8] and need corrosion protection.

Research has been carried out to improve their corrosion resistance, either by adding alloying elements [2–5], or by applying protective coatings [6,9–12]. Much has been published on the role of organic and metallic coatings on the corrosion protection of sintered NdFeB magnets [9–12]. However, the literature on the effect of conversion coatings on the corrosion resistance of these types of magnets is scarce. Only recently, phosphating of NdFeB magnets and its effect on their corrosion resistance has been studied [13–16]. The phosphate layer could also have a beneficial effect on adhesion of organic coatings to NdFeB magnets. In addition, phosphating has no

significant effect on magnetic properties, or dimension of magnets, as very thin layers, below  $1 \mu\text{m}$ , are formed.

Phosphating is an environmentally friendly surface treatment, often used as pretreatment prior to coatings application. Besides, the conversion coating resulting from phosphating can be improved by the incorporation of other protective species into the coating. It is well known that chromating is the most effective conversion coating treatment, however, its use has been drastically reduced in recent years due to its toxicity.

Recent works have reported the use of anodic inhibitors, among them tungstate and molybdate anions, which improve the film resistance and hinder the pit propagation process in iron and steel [17–19]. Moreover, investigations have shown increased coating performance of molybdate conversion layers on aluminium alloys [20,21]. Concerning the NdFeB magnets there is no data in the literature about conversion layers produced by using these anodic inhibitors.

The purpose of this work is to study the effect of various surface treatments consisted of phosphating and phosphating with tungstate incorporation on the corrosion resistance of sintered NdFeB magnets. Some of the magnets surface were

\* Corresponding author. Tel.: +55 51 3316 6292.

E-mail address: [denise@iq.ufrgs.br](mailto:denise@iq.ufrgs.br) (D.S. Azambuja).

phosphated in a solution made of  $10 \text{ g L}^{-1} \text{ NaH}_2\text{PO}_4$ , acidified to pH 3.8, and others were phosphated in the same solution, and then immersed in a  $0.1 \text{ mol L}^{-1} \text{ Na}_2\text{WO}_4$  solution during 72 h at open circuit potentials (OCP), before being tested for corrosion resistance. The corrosion resistance of the coated NdFeB magnets by was evaluated in aerated  $0.10 \text{ mol L}^{-1} \text{ Na}_2\text{SO}_4$  solution, using electrochemical impedance spectroscopy (EIS) and cyclic voltammetry.

## 2. Experimental procedure

### 2.1. Material

The material used in this study was a NdFeB commercial magnet produced by a powder metallurgical route and supplied by CRUCIBLE Co. (known as Crumax). The chemical composition of the magnet is given in Table 1.

The hydrostatic density of the NdFeB magnets used in this study is  $7.58 \text{ g cm}^{-3}$  whereas their theoretical density is  $7.60 \text{ g cm}^{-3}$ .

### 2.2. Specimen preparation and experimental set-up

Disc working electrodes with area of approximately  $1.3 \text{ cm}^2$  were prepared from the NdFeB magnet by cold resin (epoxy) embedding. The surface was prepared by grinding with silicon carbide paper up to grade #2000, followed by degreasing with alcohol, using an ultrasonic bath, and drying under a hot air stream.

A saturated calomel electrode (SCE) was used as reference electrode and all potentials are referred to it. The auxiliary electrode was a Pt gauze. The experiments were carried out under naturally aerated conditions at  $25 \text{ }^\circ\text{C}$ . The electrochemical measurements were performed using a potentiostat (AUTOLAB PGSTAT 30) coupled to a frequency response analyses (FRA 2) system and an analytical rotator PAR 616.

The EIS measurements were performed in potentiostatic mode at the open circuit potential, OCP. The OCP after potential stabilization is referred in this work as the corrosion potential,  $E_{\text{corr}}$ . The amplitude of the EIS perturbation signal was 10 mV, and the frequency range studied was from  $10^5$  to  $10^{-2} \text{ Hz}$ .

### 2.3. Conversion coating treatment

Phosphate conversion coating treatment was carried out by immersion of the magnets in a solution made of  $10 \text{ g L}^{-1} \text{ NaH}_2\text{PO}_4$ , acidified with  $\text{H}_3\text{PO}_4$  to pH 3.8, for up to 24 h.

Experiments were performed to investigate the effect of the incorporation of tungstate into the phosphate layer, by immersion of the phosphated magnets in  $\text{Na}_2\text{WO}_4$  solutions. Initially,

the effect of tungstate as a corrosion inhibitor for the phosphated magnet was investigated by adding  $x \text{ mol L}^{-1}$  ( $0 \leq x \leq 0.1$ ) of  $\text{Na}_2\text{WO}_4$  to the corrosion test solution ( $0.1 \text{ mol L}^{-1} \text{ Na}_2\text{SO}_4$ ). Subsequently, the effect of tungstate incorporation into the phosphate layer on the magnet's corrosion resistance was also studied. For this purpose, some of the phosphated specimens were re-immersed in a  $0.1 \text{ mol L}^{-1} \text{ Na}_2\text{WO}_4$  solution for 72 h at OCP under naturally aerated conditions at  $25 \text{ }^\circ\text{C}$ . After this period, the surfaces of the magnets were rinsed, dried and finally corrosion tested in a  $0.1 \text{ mol L}^{-1} \text{ Na}_2\text{SO}_4$  solution.

## 3. Results and discussion

### 3.1. Effect of phosphating

Table 2 shows a comparison between the results obtained for the untreated and the phosphated alloy after 1 h immersion in  $0.1 \text{ mol L}^{-1} \text{ Na}_2\text{SO}_4$  solution at the open circuit potential, at static and dynamic conditions. The OCP for both electrodes remains in the active region, independently on the mass transport regimen. Due to the difficulty in determining the polarisation resistance, the resistive component of the impedance measured at a sufficiently low fixed frequency has been employed to evaluate the corrosion resistance of the magnet [22]. In the present work the lowest frequency used was 10 mHz, and the resistance at this frequency ( $R_{10 \text{ mHz}}$ ) was used to qualitatively indicate the magnet's corrosion resistance.

The phosphated magnet exhibited the highest resistance at 10 mHz ( $R_{10 \text{ mHz}}$ ) for static but not for dynamic conditions. This feature can be ascribed to loss of adherence of the phosphated layer under dynamic conditions, exposing the bare surface to the electrolyte. The Nyquist plots of the phosphated magnet in  $0.1 \text{ mol L}^{-1} \text{ Na}_2\text{SO}_4$  solution at  $\omega=0$  and  $\omega=1000 \text{ rpm}$  are shown in Fig. 1. The results reveal that under rotation, the capacitive semicircle decreases significantly, and this was probably due to increase in the corroding area. The depressed capacitive loops are related to frequency dispersion due to defects in the phosphated layer and/or heterogeneities on the surface of sintered magnet [23].

### 3.2. Effect of tungstate addition in the electrolyte (test) solution

A previous set of experiments was carried out to evaluate the corrosion inhibiting effect of sodium tungstate addition to  $0.1 \text{ mol L}^{-1} \text{ Na}_2\text{SO}_4$  electrolyte.

Cyclic voltammograms were obtained with the untreated NdFeB electrode in  $0.10 \text{ mol L}^{-1} \text{ Na}_2\text{SO}_4$  solution containing  $x \text{ mol L}^{-1}$  of tungstate ( $0 \leq x \leq 0.1$ ) at  $0.020 \text{ V s}^{-1}$  and  $\omega=0$  (Fig. 2). Passivity breakdown took place in tungstate containing electrolytes at tungstate concentrations lower than  $0.075 \text{ mol L}^{-1}$ , regardless the electrode rotation (data not shown). Once the film had broken down and pitting corrosion started, drastic dissolution of the alloy occurred (curves a and b).

Similar voltammograms were obtained with the phosphated alloy and these are shown in Fig. 3. As can be seen in this last Figure, the addition of  $0.03 \text{ mol L}^{-1} \text{ Na}_2\text{WO}_4$  to the sulphate

Table 1  
Chemical composition of commercial Nd–Fe–B magnets

Element	Fe	Nd	B	Dy	Al	Co	Si	Cu	Nb
Wt.%	60.9	28.6	1.0	2.1	3.8	1.3	1.4	0.2	0.7
At.%	67.9	12.3	5.8	0.8	8.1	1.4	3.1	0.2	0.4

Table 2

Corrosion potential ( $E_{\text{corr}}$ ) and resistance ( $R_{10 \text{ mHz}}$ ) of the untreated and phosphated NdFeB at static ( $\omega=0 \text{ rpm}$ ) and dynamic ( $\omega=1000 \text{ rpm}$ ) conditions after 1 h of immersion in  $0.1 \text{ mol L}^{-1} \text{ Na}_2\text{SO}_4$  solution

	$E_{\text{corr}}$ (V)	$R_{10}$ ( $\Omega \text{ cm}^2$ )
Static conditions		
Untreated magnet	-0.76	890
Phosphated magnet	-0.71	1760
Dynamic conditions		
Untreated magnet	-0.74	88
Phosphated magnet	-0.66	835

solution leads to passivation of the phosphated alloy. This behaviour evidences that the phosphating treatment produces a surface with a reduced number of active dissolution sites, which can be repaired in the presence of tungstate anions. No significant changes were detected for the cyclic voltammograms performed under electrode rotation in tungstate containing solutions.

Electrochemical impedance measurements carried out at the corrosion potential for the phosphated magnet after 1 h of immersion in sulphate solution containing  $x \text{ mol L}^{-1} \text{ Na}_2\text{WO}_4$  ( $x=0.01; 0.03; 0.05$ ), are shown in Fig. 4. On increasing tungstate concentration, it was observed that the two capacitive loops are overlapped ( $R_{10 \text{ mHz}}$  increases), being ascribed to the tungstate adsorption on the electrode surface [24].

In order to evaluate the effect of electrode rotation in the presence of tungstate ions on the magnet's electrochemical behaviour, tests were also performed at 1000 rpm for the phosphated alloy in  $0.1 \text{ mol L}^{-1} \text{ Na}_2\text{SO}_4$  solution with  $0.05 \text{ mol L}^{-1} \text{ Na}_2\text{WO}_4$  (data not shown). At static conditions,  $E_{\text{corr}}$  reaches a stable potential of  $-0.33 \text{ V}$  whereas under electrode rotation (1000 rpm),  $E_{\text{corr}}$  stabilized at  $-0.38 \text{ V}$ . Under electrode rotation,  $R_{10 \text{ mHz}}$  and the phase angle increases, and this is probably due to the enhanced flux of dissolved oxygen to the

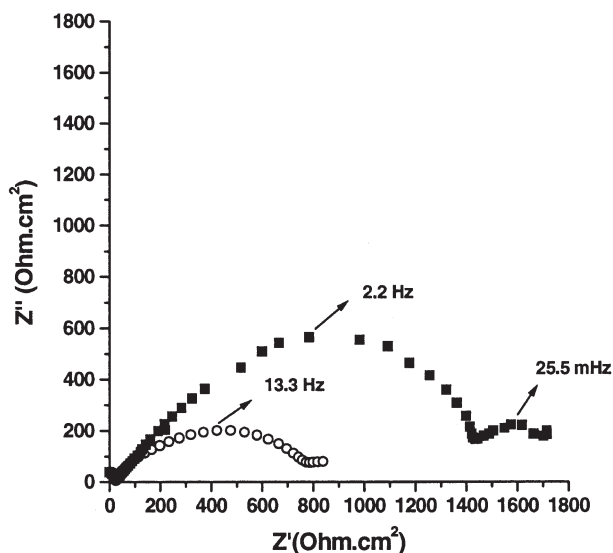


Fig. 1. Nyquist plots of phosphated magnet at OCP after 1 h immersion in  $0.1 \text{ mol L}^{-1} \text{ Na}_2\text{SO}_4$  at  $\omega=0$  (■) and  $\omega=1000 \text{ rpm}$  (○).

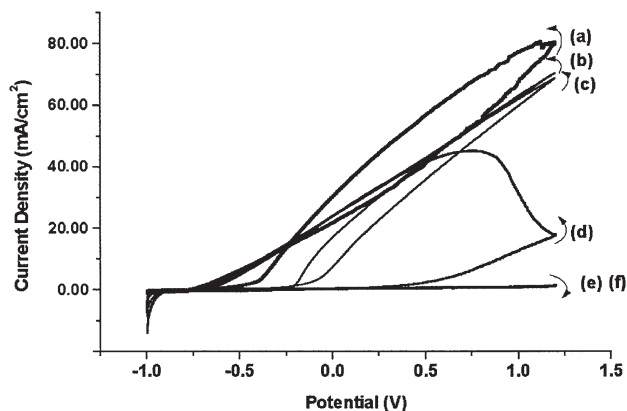


Fig. 2. Cyclic voltammograms for untreated NdFeB electrode in  $0.10 \text{ mol L}^{-1} \text{ Na}_2\text{SO}_4$  and  $x \text{ mol L}^{-1} \text{ Na}_2\text{WO}_4$  solution from  $-1.0$  to  $+1.2 \text{ V}$  at  $v=0.020 \text{ V s}^{-1}$  at  $\omega=0$ : (a)  $x=0.0$ ; (b)  $x=0.01$ ; (c)  $x=0.03$ ; (d)  $x=0.05$ ; (e)  $x=0.075$  and (f)  $x=0.10$ .

electrode surface, favoring film repair in the presence of tungstate anions [18,19]. The effect of rotation on corrosion inhibition may be related to one or more of the following influences resulting from increased mass transport: (i) easier adsorption of the inhibiting species owing to their higher concentration at the surface; (ii) higher oxygen concentration at the magnet surface; (iii) decreased local acidification due to consumption of the  $\text{H}^+$  ions produced in the hydrolysis of metallic cations by tungstate anions.

The effect of immersion time of the phosphated magnet in tungstate containing solution ( $0.10 \text{ mol L}^{-1} \text{ Na}_2\text{SO}_4$  with  $0.10 \text{ mol L}^{-1} \text{ Na}_2\text{WO}_4$ ) was also evaluated and the EIS spectra at various immersion times in this last solution are shown in Fig. 5. The diagrams show two time constants, corresponding to both capacitive and diffusional processes.  $E_{\text{corr}}$  remained stable at approximately  $-0.32 \text{ V}$  up to 222 h corresponding to the active to passive transition region. On the other hand, the corrosion resistance is enhanced by the action of tungstate anion, due to its adsorption on the exposed magnet surface at

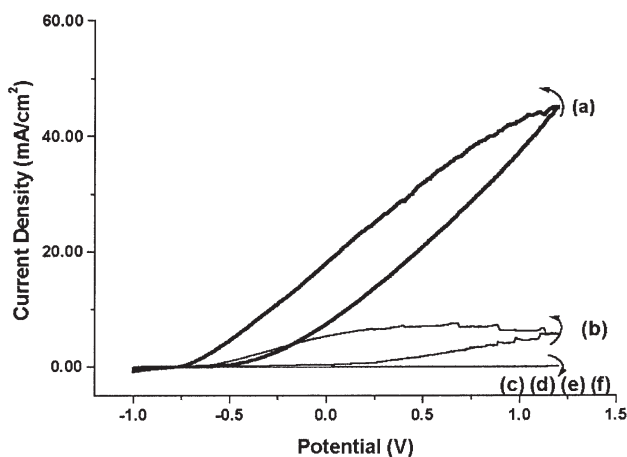


Fig. 3. Cyclic voltammograms for phosphated NdFeB electrode in  $0.10 \text{ mol L}^{-1} \text{ Na}_2\text{SO}_4$  and  $x \text{ mol L}^{-1} \text{ Na}_2\text{WO}_4$  solution, from  $-1.0$  to  $+1.2 \text{ V}$  at  $v=0.020 \text{ V s}^{-1}$  at  $\omega=0$ . (a)  $x=0.0$ ; (b)  $x=0.01$ ; (c)  $x=0.03$ ; (d)  $x=0.05$ ; (e)  $x=0.075$  and (f)  $x=0.10$ .

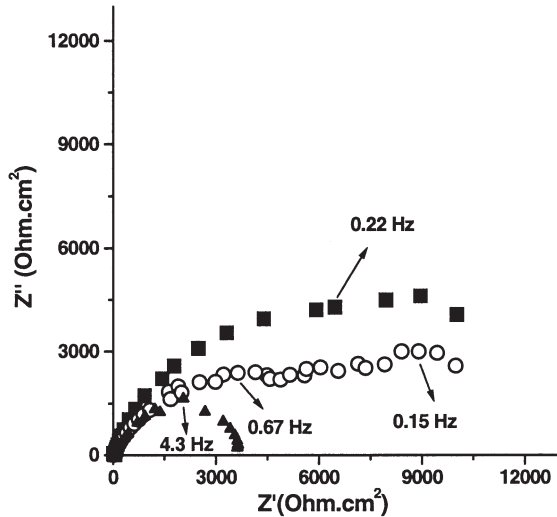


Fig. 4. Nyquist plots for phosphated NdFeB electrodes at OCP after 1 h of immersion in  $0.10 \text{ mol L}^{-1} \text{ Na}_2\text{SO}_4$  and  $x \text{ mol L}^{-1} \text{ Na}_2\text{WO}_4$  solution, at  $\omega = 0$ . (▲)  $x = 0.01$ ; (○)  $x = 0.03$ ; (■)  $x = 0.05$ .

uncovered areas, repairing the defects in the coating and consequently, leading to a more protective layer.

### 3.3. The effect of tungstate incorporation into phosphate conversion layer

Based on the results presented in the previous section, tests were also performed by immersion of the phosphated magnet in tungstate containing solution to evaluate the incorporation of these anions into the conversion coating. Two sodium tungstate ( $\text{Na}_2\text{WO}_4$ ) concentrations were tested,  $0.05 \text{ mol L}^{-1}$  and  $0.1 \text{ mol L}^{-1}$ . No beneficial effects were detected by the treatment in the  $0.05 \text{ mol L}^{-1} \text{ Na}_2\text{WO}_4$  solution (data not shown). Thus, the  $0.1 \text{ mol L}^{-1} \text{ Na}_2\text{WO}_4$  solution was used for incorporation of tungstate. For this purpose, two surface treatments were

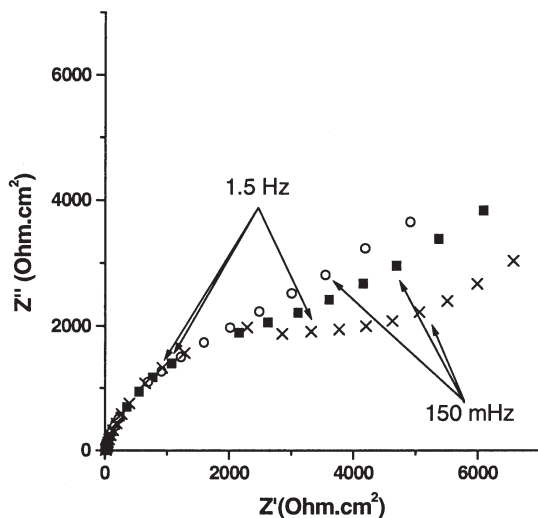


Fig. 5. Nyquist plots for phosphated NdFeB electrode at OCP in  $0.10 \text{ mol L}^{-1} \text{ Na}_2\text{SO}_4$  solution containing  $0.10 \text{ mol L}^{-1} \text{ Na}_2\text{WO}_4$ , at  $\omega = 0$  after 48 (×), 164 (■) and 212 (○) h of immersion.

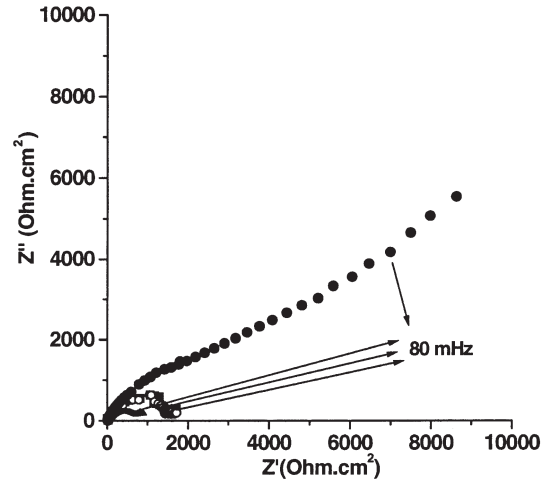


Fig. 6. Nyquist plots for NdFeB magnet at OCP after 1 h immersion in  $0.10 \text{ mol L}^{-1} \text{ Na}_2\text{SO}_4$ . Magnet (▲) untreated, (■) phosphated, (○) phosphated+treatment 1, (●) phosphated+treatment 2.

performed, either by immersing the phosphated magnets in the tungstate solution under anodic polarization at  $0.20 \text{ V}$  for 1 h (treatment 1) or by immersion in the tungstate solution at open circuit conditions during 72 h (treatment 2). Fig. 6 shows the Nyquist plots for untreated and phosphated magnets after treatments 1 and 2, obtained after 1 h of immersion in  $0.10 \text{ mol L}^{-1} \text{ Na}_2\text{SO}_4$  solution. As it can be seen, the resistance of the magnet after treatment 1 remains unaltered and its  $E_{\text{corr}}$  is approximately  $-0.65 \text{ V}$ . On the other hand, the magnet after treatment 2, presented  $E_{\text{corr}}$  values around  $-0.10 \text{ V}$ , corresponding to its passive region. A comparison of  $R_{10 \text{ mHz}}$  values for the phosphated magnet (Table 2) and for the phosphated magnet after treatment 2 shows that this last treatment increases  $R_{10 \text{ mHz}}$  by approximately seven times, from  $1.76$  to  $12.4 \text{ k}\Omega \text{ cm}^2$ . This result can be attributed to the incorporation of tungstate in the defects of the phosphate layer, enhancing magnet's corrosion resistance, even at prolonged immersion times (up to 4 days). The  $R_{10 \text{ mHz}}$  values were stable (approximately  $11.5 \text{ k}\Omega \text{ cm}^2$ ) during this period (data not shown here).

The EIS plots show two a depressed a capacitive loop at high frequencies and a diffusional processes at low frequency region. The maximum phase angle of all diagrams (Bode plots), near  $-45^\circ$ , can be ascribed to a Warburg impedance (data not given here).

The equivalent circuit (EC) proposed for fitting the EIS diagrams shown in Fig. 6 is  $R_s(Q[R_pW])$ . In the proposed EC (Fig. 7)  $R_s$  represents the ohmic resistance between reference

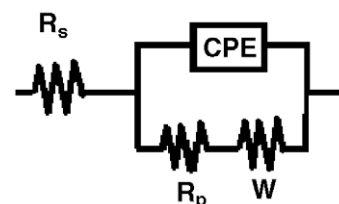


Fig. 7. Equivalent circuit proposed for fitting the EIS diagrams shown in Fig. 7.

Table 3  
Equivalent circuit elements obtained from fitting experimental data to the equivalent circuit proposed to simulate untreated and phosphated magnet surfaces and shown in Fig. 6

Treatment	$E_{\text{corr}}$ (mV)	$R_S$ ( $\Omega \text{ cm}^2$ )	$Q$ ( $\mu\text{F cm}^{-2}$ )	$n$	$R_p$ ( $\Omega \text{ cm}^2$ )	$W$ ( $\Omega^{-1} \text{ cm}^{-2}$ )
(1) Mechanical grinding with SiC paper to #1200	-0.76	17.7	5.1	0.59	890	$0.31 \times 10^{-1}$
(2) As (1)+phosphating	-0.71	25.8	29	0.66	1076	$0.39 \times 10^{-2}$
(3) As (1)+phosphating+treatment 1	-0.65	18.8	4.8	0.71	1551	$0.14 \times 10^{-1}$
(4) As 1+phosphating+treatment 2	-0.10	17.4	2.1	0.77	9570	$0.11 \times 10^{-3}$

and working electrodes,  $R_p$  represents the polarization resistance,  $Q$  is the impedance related to a constant phase element (CPE) and  $W$  is the diffusional Warburg impedance. The capacitance was replaced by a CPE impedance, which takes into account the phenomena related to surface roughness and inhomogeneous. The CPE impedance is given by [26]:

$$Z_{\text{CPE}} = [Q(j\omega)^n]^{-1}$$

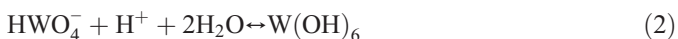
where CPE represents an ideal capacitor for  $n=1$ , a resistor for  $n=0$  and diffusional processes if  $n=0.5$ . The Warburg impedance was introduced due to mass transport processes [25] within the pores and defects of the coating. The fitting quality was judged based on the error percentage associated to each component. The fitted data in Table 3 show errors smaller than 5%.

The deviation from the ideal behaviour of a capacitor ( $n$  values lower than 1 were obtained) is associated to surface defects. The magnet used in this study was produced by powder metallurgy and, consequently, presents an inhomogeneous surface with porosities and a combination of different phases [13].

The results show evidence that immersion of phosphated magnets in tungstate solution (treatment 2) improves their corrosion resistance. The lowest CPE value and the  $n$  exponent close to 0.77, as well the Warburg impedance decrease obtained with these electrodes, indicate that the incorporation of tungstate in the phosphate layer produces a more protective film.

The lower  $R_{10 \text{ mHz}}$  values obtained with treatment 1 (under anodic polarization at 0.2 V), can be explained as follows. Despite the decrease in coating porosity ( $n=0.71$ ) after treatment in tungstate containing solution, a number of active sites remain on the surface. Hence, under anodic polarization, competitive processes take place on the electrode surface, being the dissolution rate at the uncovered areas higher than that of the tungstate charge transfer reaction [27].

The higher corrosion resistance obtained for phosphated magnets immersed in the  $0.1 \text{ mol L}^{-1}$  tungstate solution during 72 h at OCP (treatment 2) can be related to three premises. First, tungstate anions show buffering properties [28] consuming the  $\text{H}^+$  ions produced in the hydrolysis of metallic cations, and suppressing the local acidification according to the following reactions:



Second, several tungstate polymeric species, such as:  $\text{W}_{10}\text{O}_{32}^{4-}$ ,  $\text{H}_2\text{W}_{12}\text{O}_{40}^{6-}$ ,  $\text{H}_2\text{W}_{12}\text{O}_{42}^{10-}$  [28–30] are formed with metallic cations which can be adsorbed on the metal surface

and on the coating, repairing defects and producing a more protective film. Third, the adsorption of tungstate anions on iron and steel electrodes follows a slow kinetic rate, as previously reported [18]. Consequently, long exposure times (72 h) lead to increasing blockage of the metallic substrate exposed at defects in the coating. Another point that must be considered concerns the phosphate solution, which acts by promoting surface passivation and also its repassivation in sites where film breakdown takes place [16]. Hence, it can be postulated that a synergistic effect was obtained by treatment 2, considerably improving the corrosion resistance of the magnet, if compared to the results obtained with the phosphating treatment. It was demonstrated that the magnet submitted to treatment 2 have shown a higher protective character even in the aggressive media used in this study ( $0.1 \text{ mol L}^{-1} \text{ Na}_2\text{SO}_4$ ).

#### 4. Conclusions

The results obtained revealed that the corrosion resistance of sintered NdFeB magnet is greatly improved by the tungstate incorporation into the phosphate conversion coating resulting from a phosphating treatment prior to immersion in the tungstate solution. The proposed treatment consists of phosphating of NdFeB by immersion in a solution of  $10 \text{ g L}^{-1} \text{ NaH}_2\text{PO}_4$ , acidified to pH 3.8, followed by re-immersion of the phosphated magnet in a  $0.1 \text{ mol L}^{-1} \text{ Na}_2\text{WO}_4$  solution for 72 h at OCP conditions. Corrosion tests carried out in  $0.1 \text{ mol L}^{-1} \text{ Na}_2\text{SO}_4$  solution indicated that the increased protective nature of the surface layer after immersion in tungstate solution is due to the adsorption of tungstate at the metallic substrate exposed under defects/pores in the coating, impeding metal dissolution in the pores/defects and preventing localized corrosion propagation.

#### Acknowledgments

Financial support to this work by Brazilian agencies CNPq, CAPES, FAPERGS and FAPESP are gratefully acknowledged.

#### References

- [1] G.W. Warren, G. Gao, Q. Li, J. Appl. Phys. 70 (1991) 6609.
- [2] S. Hirose, S. Mino, H. Tomizawa, J. Appl. Phys. 69 (1991) 5844.
- [3] K. Tokuhara, S. Hirose, J. Appl. Phys. 69 (1991) 5521.
- [4] M. Sagawa, P. Tenaud, F. Vial, K. Hiraga, IEEE Trans. Magn. 26 (1990) 1957.
- [5] E. Rozendall, IEEE Trans. Magn. 26 (1990) 2631.
- [6] H. Bala, G. Pawlowska, S. Szymura, Y.M. Rabinovich, Br. Corros. J. 33 (1998) 37.

- [7] A.S. Kim, F.E. Camp, *J. Appl. Phys.* 79 (1996) 5035.
- [8] C.W. Cheng, F.T. Cheng, *J. Appl. Phys.* 83 (1998) 6417.
- [9] C.D. Qin, A.S.K. Li, D.H.L. Ng, *J. Appl. Phys.* 79 (1996) 4854.
- [10] F.H. Firsching, J.C. Kell, *J. Chem. Eng. Data* 38 (1993) 132.
- [11] E. Pierrì, D. Tsamouras, E. Dalas, *J. Cryst. Growth* 213 (2000) 93.
- [12] I. Costa, I.J. Sayeg, R.N. Faria, *IEEE Trans. Magn.* 33 (1997) 3907.
- [13] A.M. Saliba-Silva, I. Costa, *Key, Eng. Mater.* 189–191 (2001) 363.
- [14] A.M. Saliba-Silva, H.G. de Melo, M.A. Baker, A.M. Brown, I. Costa, *Mater. Sci. Forum* 416 (2003) 76.
- [15] A.M. Saliba-Silva, PhD thesis, University of Sao Paulo, Brazil, 2001.
- [16] A.M. Saliba-Silva, R.N. Faria, M.A. Baker, I. Costa, *Surf. Coat. Technol.* 185 (2004) 321.
- [17] H. Fujioka, K. Nishihara, Aramaki, *Corros. Sci.* 38 (1996) 1915.
- [18] J.M. Abd El Kader, A.A. El Warraky, A.M. Abd El Aziz, *Br. Corros. J.* 33 (1998) 139.
- [19] D.S. Azambuja, E.M.A. Martini, I.L. Muller, *J. Braz. Chem. Soc.* 14 (2003) 570.
- [20] J.D. Gorman, S.T. Jonhson, P.N. Jonhtson, P.J.K. Paterson, A.G. Hughes, *Corros. Sci.* 38 (1996) 1957.
- [21] J.D. Gorman, S.T. Jonhson, P.N. Jonhtson, P.J.K. Paterson, A.G. Hughes, *Corros. Sci.* 38 (1996) 1977.
- [22] A.A.O. Magalhães, I.C.P. Margarit, O.R. Mattos, *Electrochim. Acta* 44 (1999) 4281.
- [23] E.M.A. Martini, S.T. Amaral, I.L. Muller, *Corros. Sci.* 46 (2004) 2097.
- [24] F. Deflorian, L. Fedrizi, A. Locaspi, P.L. Bonora, *Electrochim. Acta* 38 (1993) 1945.
- [25] G.W. Walter, *Corros. Sci.* 26 (1986) 681.
- [26] A. Losch, J.W. Schultze, *J. Electroanal. Chem.* 359 (1983) 39.
- [27] H.S. Isaacs, *Corros. Sci.* 29 (1989) 313.
- [28] F.A. Cotton, G. Wilkinson, *Advanced Inorganic Chemistry*, 5th ed. John Willey and Sons, New York, 1988.
- [29] M. Sakashita, N. Sato, *Corros. Sci.* 17 (1977) 461.
- [30] H. Fujioka, K. Nishihara, Aramaki, *Corros. Sci.* 38 (1996) 1915.